Laser-Power-Induced Multiphonon Resonant Raman Scattering in Laser-Heated CdS Nanocrystal

Satyaprakash Sahoo* and A. K. Arora

Condensed Matter Physics Division, Indira Gandhi Centre for Atomic Research, Tamil Nadu 603102, India

Received: December 22, 2009; Revised Manuscript Received: February 19, 2010

The size stability of nanoparticles is crucial from an application point of view. We probe, using Raman spectroscopy, particle size evolution of CdS nanoparticles by varying laser power. Multiphonon resonant Raman scattering has also been demonstrated. With increase in laser power, the intensity ratio of 2-longitudinal optical (LO) to 1-LO is found to increase dramatically, and LO phonon overtones up to fourth order are observed. Resonant Raman scattering has been achieved by suitably matching the band gap with the excitation photon energy, by varying the local temperature. The effect of increase in local temperature on the band gap is also discussed.

Semiconductor materials in the nanoscale regime have been of great research interest in recent years. This is because of their promising applications in many areas which include optoelectronic devices, solid-state lasers, and solar cells.[1−3] There are several techniques to fabricate semiconductor-based electronic devices; laser-induced doping is one among them. Moreover, localized heating can give rise to change in nanocrystal size and phase which can significantly alter various properties, in particular, at the interface where a large difference in size or phase can modify the properties of an otherwise homogeneous structure. Among semiconductor materials, CdS nanostructures in the form of quantum dots, nanowires, and thin films are widely investigated by many researchers.[4−6] Recently, Yakovlev et al. have demonstrated the effect of pulse laser radiation on the structural phase change in CdS nanoparticles.[7] One can study laser-induced structural changes by Raman spectroscopy. On the other hand, room temperature resonant Raman scattering has been reported to probe the electronic state in CdS nanowires by matching the excitation energy with the band gap of CdS.[8] Electron−phonon interaction has a vital influence on the electronic properties and optical properties of semiconductor nanomaterials and is of great importance for device applications.[9] Here, we investigate the effect of laser power on the particle size evolution in CdS nanocrystals by Raman spectroscopy. Laser-power-induced multiphonon resonant Raman scattering in the localized area in CdS nanocrystals has also been reported in detail, and a theoretical temperature dependent band gap has been employed to understand multiphonon resonance.

CdS nanocrystals were synthesized at room temperature by simple chemical precipitation route in aqueous medium, which is similar to the method followed in our previous report with a small modification. For CdS nanoparticles, aqueous solutions of $Cd(CH_3COO)_2$ (0.5 mmol) were prepared. While stirring this solution at a slightly elevated temperature, 25 mL of Na_2S (0.5 mmol) aqueous solution was added which resulted in the precipitation of CdS particles. The precipitates were removed after washing with water several times and dried. CdS nanoparticles were characterized by X-ray powder diffraction using a (STOE) X-ray diffractometer for obtaining average particle size. The Raman scattering measurements were carried out using the 532 nm line of a diode-pumped solid-state laser as the excitation source and analyzed using a double-monochromator (Jobin-Yvon U1000), equipped with liquid-nitrogen-cooled CCD detector. Room temperature photoluminescence was recorded using a SPEX monochromator, and the 488 nm line of an Ar ion laser was used as the excitation source. The UV−visible absorption spectrum was recorded using a Jasco V 650 spectrometer in which a xenon lamp was used as the excitation source.

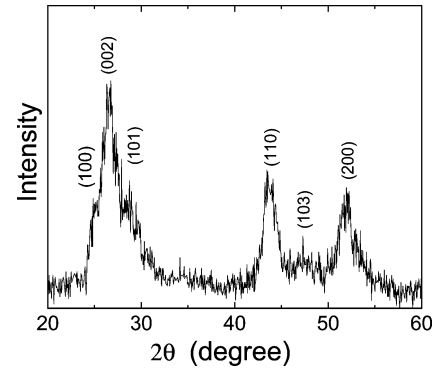

Figure 1. X-ray diffraction pattern of as-synthesized wurtzite CdS nanocrystals.

Powder XRD shows broad and distinct peaks that match that of JCPDS data for the wurtzite phase of CdS as shown in Figure 1. The average particle size was estimated using Scherrer's formula and was found to be 4 nm. Figure 2 shows the Raman spectrum of CdS nanoparticles using 532 nm (2.33 eV) excitation energy at the lowest laser power of 1 mW. The spectrum shows the most intense peak at 297 cm^{-1} and a less intense peak at 594 cm^{-1}. These peaks have been assigned as 1-longitudinal optical (LO) and 2-LO, respectively, as reported for bulk CdS data.[10] It may be pointed out that no other higher order LO modes have been observed. The inset shows the 1-LO phonon modes of CdS nanoparticles excited with different laser powers. The size of the laser spot was about 100 μm. The corresponding local

* Author to whom correspondence should be addressed. E-mail: satyasahoo@igcar.gov.in, satya504@gmail.com. Phone: 044-27480081. Fax: 044-27480081.

10.1021/jp912103t
Published on Web 03/05/2010

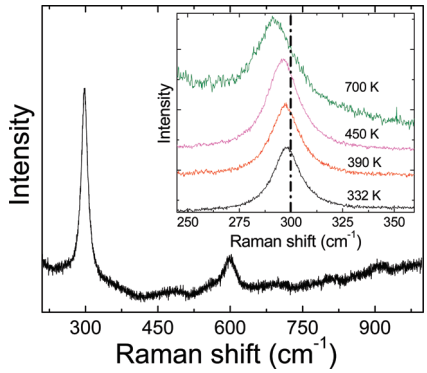

Figure 2. Raman spectra of as-synthesized CdS nanoparticles recorded at lowest laser power. The inset shows the 1-LO spectra at different local temperature obtained by varying the laser power.

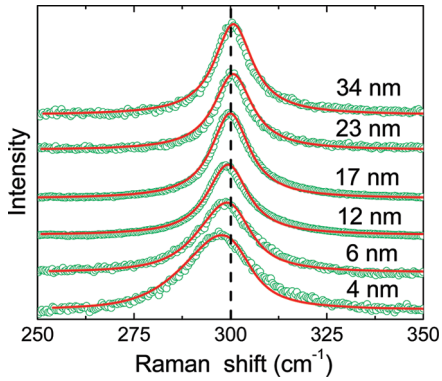

Figure 3. Comparison of calculated and measured Raman line shapes for the 1-LO phonon of CdS nanocrystals. Open symbols are the room temperature data, and solid curves are calculated using the phonon confinement model.

temperatures are calculated by taking the Stoke to anti-Stoke intensity ratio as follows[11]

$$\frac{I_s}{I_{as}} = K \exp\left(\frac{\hbar\omega}{k_B T}\right) \tag{1}$$

where I_s and I_{as} are the Stoke and anti-Stoke intensity. At room temperature, the 1-LO phonon appears at 297 cm^{-1} and the full width at half-maximum (fwhm) is found to be 19 cm^{-1} in contrast to bulk CdS where 1-LO appears at 301 cm^{-1} and fwhm is 12 cm^{-1}.[10] The red shift of LO phonon frequency and broadening of Raman line shape can be attributed to confinement of the optical phonon in CdS nanocrystals.[11,12] With further increase in laser power, the 1-LO phonon shows systematic red shift and broadening. The 1-LO phonon spectra recorded at different laser powers/temperatures are shown as the inset in Figure 2. The laser power dependent phonon modes have been reported for TiO_2 nanocrystals and Si nanowires.[11−13] Here we want to mention that room temperature Raman spectra (at the lowest power 1 mW) were also recorded each time after the laser power was increased as shown in Figure 3. The peak position and fwhm of these room temperature spectra are compared with the spectra obtained for the as-synthesized sample at 1 mW. This is because a deviation in the comparison will give an idea about the temperature at which the particle size starts increasing. A phonon confinement model was used to analyze these room temperature spectra to estimate the particle size.[11] This will be discussed in detail later. It is important to note that an increase in local temperature up to 450 K (75 mW laser power) does not affect the size of the nanoparticles. Recently it has been reported that substantial grain growth takes place above 450 K.[14] Laser heating can also cause oxidation of the surface resulting in formation of CdO. It has been reported that CdS oxidizes at about 873 K.[15] This temperature is well above the highest temperature obtained (700 K) in the present study. In addition, the laser heating was done for a short time, probably not sufficient for oxidation. Only prolonged heating is known to cause oxidation. The absence of Raman mode associated with CdO in the present study indicates that CdO phase is not formed.

Analysis of phonon confinement to estimate the particle size is in order. In the case of perfect crystals, only the optical phonons at the zone center are involved in the first-order Raman scattering process. This is because of the fact that the momentum conservation rule is valid in perfect crystals. However, in the case of nanocrystals, the lattice periodicity is interrupted at the particle surface and the phonon gets confined within the nanocrystals. Thus the phonon wave function has to decay to a small value close to the boundary. This restriction on the phonon wave function in the real space, via a relaxation of the selection rule, allows a range of q vectors up to $\Delta q \sim \pi/d$ (d is the particle size) in the Brillouin zone to contribute to Raman scattering, resulting in a shift as well as broadening of the Raman peak. Different approaches have been used to theoretically investigate the consequences of confinement on phonon spectra. In analogy with the spatial correlation model, originally developed for disordered and amorphous materials, a Gaussian confinement model was proposed by Campbell and Fauchet.[16] This model has been extensively used to explain the Raman line shape of various nanocrystals. According to this model the intensity of first-order Raman scattering for a nanocrystal of diameter d is

$$I(\omega, d) = \int \frac{|C(q,d)|^2}{[\omega - \omega(q)]^2 + (\Gamma_0/2)^2} d^3q \tag{2}$$

where $\omega(q)$ is the phonon dispersion curve and Γ_0 is the natural line width of zone-center optical phonon in bulk anatase. $C(q, d)$ is the Fourier transformation of the confinement function and is given by

$$|C(q,d)|^2 = \exp\left(\frac{-q^2 d^2}{2\alpha}\right) \tag{3}$$

A large number of results have been satisfactorily explained on the basis of the Gaussian confinement model using $\alpha = 8\pi^2$. If Δ is the width of the dispersion curve of the optical phonon, then the dispersion curve can be approximated as

$$\omega(q) = \omega_0 - \Delta \sin^2\left(\frac{qa}{2}\right) \tag{4}$$

where ω_0 is the zone-center optical phonon frequency and a is the lattice parameter. The values of Γ_0, Δ, ω_0, and a that are used in the calculations are 12, 35, and 301 cm^{-1} and 4.13 Å, respectively. Figure 3 shows the comparison between measured and calculated Raman line shape for different particle sizes. The particle sizes estimated are 6, 8, 12, 17, 22, 28, and 34 nm for laser power of 90, 100, 110, 120, 130, 140, and 150 mW, respectively. One can see there is a good agreement between measured and calculated line shapes. This suggests that as-

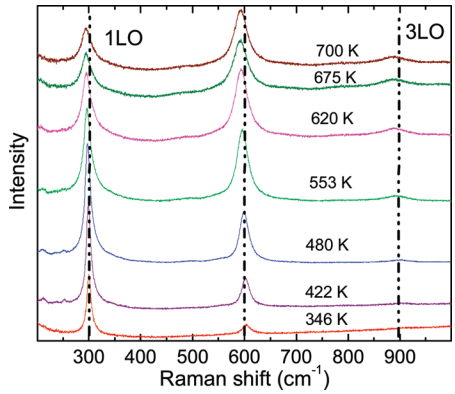

Figure 4. Raman spectra obtained by varying the laser power on the area after heating with highest laser power. The corresponding local temperatures are also indicated.

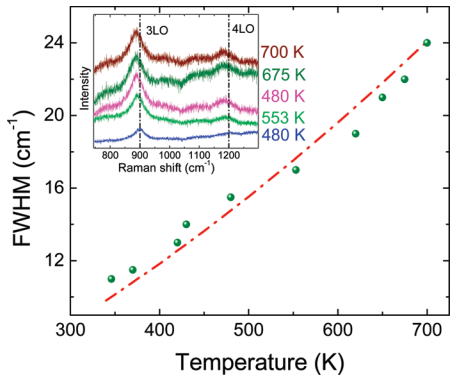

Figure 5. Variation of fwhm with temperature. The dot-dashed curve is fit to the data by adding eqs 5 and 6. The inset shows the Raman spectra of 3- and 4-LO recorded at various laser powers.

synthesized sample and the various laser-heated samples have low defect concentration.

A discussion on the mechanism of increase in particle size is in order. Particle size growth can arise either due to Ostwald ripening or due to melting and recrystallization. Nanoparticles of CdS are known to melt at lower temperature than the bulk.[17] The melting point of CdS (bulk ~ 1687 K) reduces to 1200 K for 3.5 nm particles and further to 600 K for 1.5 nm size. In view of this, one needs to examine whether any melting occurred in present laser-heating experiments. The highest local temperature achieved at highest laser power is much lower than the melting point of the smallest nanoparticles in the present work. Thus one can rule out the possibility of local melting. Furthermore, the laser heating was done on the same spot with successively higher powers. Thus the average size grew from 4 to 34 nm gradually with laser power due to Ostwald ripening.

Figure 4 shows the Raman spectra recorded at various laser powers on the area which was previously heated to a local temperature of 700 K using highest laser power. We have essentially performed the experiment on the area of the sample where particle size already increased to 34 nm. One can see that with increase in local temperature, the intensity of the 1-LO phonon keeps on decreasing, and on the other hand, the intensity of the 2-LO phonon shows an increase. Interestingly, the intensity of the 3-LO phonon at around 900 cm^{-1} starts increasing as the local temperature rises to 553 K. The effect of rise in local temperature on the peak position and line width can be seen clearly which results in broadening and red shift of LO phonon line shape. Figure 5 shows the fwhm as a function of temperature. We analyzed fwhm by using cubic and quartic anharmonicities representing three- and four-phonon processes,

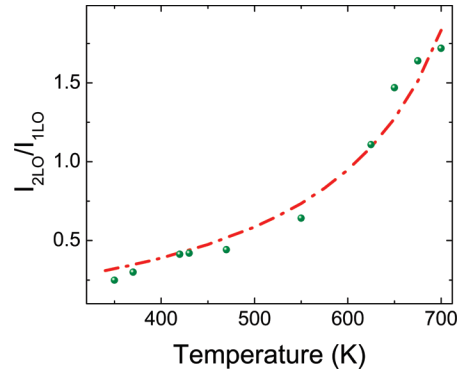

Figure 6. Variation of the ratio of the intensities of 2-LO and 1-LO with temperature. The dot-dashed curve is the *T*-dependence of the intensity ratio calculated using eq 8.

respectively. The cubic anharmonicity of the mode results in the decay of a phonon at temperature *T* into two longitudinal acoustic phonons each of equal frequency. This process results in the broadening of the Raman mode by

$$\Gamma_C = A\left\{\left[\exp\left(\frac{\hbar\omega}{2k_BT}\right) - 1\right]^{-1} + \frac{1}{2}\right\} \quad (5)$$

where *A* is the coefficient of cubic anharmonicity.[18,19] On the other hand, quartic anharmonicities result in the decay of a phonon at temperature *T* into three longitudinal acoustic phonons each of equal frequency. This process results in the broadening of the Raman mode by

$$\Gamma_Q = B\left(\left\{\left[\exp\left(\frac{\hbar\omega}{3k_BT}\right) - 1\right]^{-1} + \frac{1}{2}\right\}^2 + \frac{1}{12}\right) \quad (6)$$

where *B* is the coefficient of quartic anharmonicity anharmonicity.[18,19] The calculated temperature dependent fwhm, obtained by adding the above two contributions, is also shown in Figure 5. The values of *A* and *B* that are used to get good fit are 4.6 and 0.5, respectively. One can see that the above formalism gives a reasonable fit. It is important to note that the 4-LO phonon at 1200 cm^{-1} starts appearing at a local temperature of 553 K, and its intensity further increases with rise in local temperature, as shown in the inset of Figure 5.

Figure 6 shows the variation of intensity ratio of 2-LO to 1-LO as a function of local temperature. The ratio is found to exhibit a dramatic eightfold increase with increase in temperature. It is emphasized here that the ratio of 2-LO to 1-LO is the measure of electron−phonon interaction in semiconductors.[20,21] The size of nanocrystal has a significant effect on electron−phonon interaction. It has been demonstrated for ZnO nanocrystal that with reduction in size electron−phonon interaction decreases.[21] Variation of electron−phonon interaction in CdS nanocrystal as function of particle size has been investigated, and it is found that with increase in particle size the ratio of 2-LO to 1-LO increases.[14] However, if one uses light of different wavelengths keeping the temperature constant, then the values of the intensity ratio could differ from each other.[22]

In order to understand the increase in electron−phonon interaction and appearance of higher order LO modes with increase in laser power, one has to examine the resonant Raman scattering as a possible cause for these observations. It has been reported by several researchers in various materials that resonance Raman scattering occurs when the incoming or

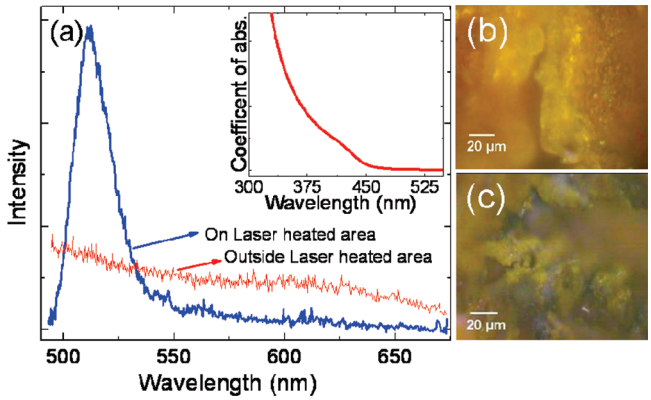

Figure 7. (a) Photoluminescence spectra of CdS nanoparticles in and outside the laser-heated area. The inset shows the absorption spectra of CdS nanoparticles. (b) and (c) are optical micrographs of outside and inside the laser-heated area of the sample, respectively.

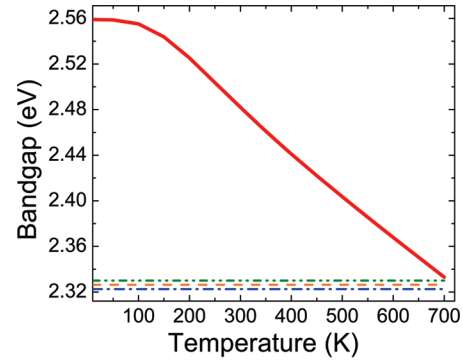

Figure 8. Variation of calculated band gap as a function of temperature. Horizontal lines from top to bottom represent the energies of incident photon (in-resonance), 1-LO scattered phonon (1-LO out-resonance), and 2-LO scattered phonon (2-LO out-resonance).

outgoing photon energy matches the band gap of the material as a result of which the intensity of the Raman spectra increases and several higher harmonics appear. This can be achieved in two ways: by tuning the photon energy close to the band gap or changing the band gap of the material close to the photon energy.[8,23,24] In the present study, the incoming photon has a fixed energy of 2.33 eV, and change in the band gap is accomplished by raising the local temperature using laser heating.

A knowledge of the band gap at the laser-heated region will be useful for understanding the electron−phonon interaction. In order to get the band gap of CdS, a photoluminescence spectrum is recorded at the laser-heated region by using a 488 nm excitation source. The spectrum recorded at room temperature is shown in Figure 7a. A distinct sharp PL peak around 2.43 eV is observed which is close to the value reported for larger nanocrystals of CdS.[25] Therefore, from the Raman and PL studies, it can be concluded that at the highest laser power large nanoparticles have formed. This result is also consistent with the particle size estimated by phonon confinement model at 700 K. For comparison, a PL spectrum of a region outside the laser-heated area was measured and is shown in Figure 7a. No PL peak is observed from this region due to the band gap of smaller nanocrystals being higher than the excitation energy. This is also confirmed by recording the absorption spectra of these nanoparticles, shown as the inset in Figure 7a. A distinct absorption edge at around 3 eV is observed. Optical micrographs of the sample outside the laser-heated area and on the laser-heated area are also shown in Figure 7b and c, respectively. A change in the color of the sample at the laser-heated area can be clearly seen. This is primarily due to the increase in particle size induced by laser heating which leads to a change in optical properties of the sample.

Now, we shall examine the variation of band gap with temperature. The temperature dependent band gap in bulk CdS is given by[26]

$$E_g(T) = E_0 - \left(\frac{\alpha T^4}{\beta + T^3}\right) \tag{7}$$

Here $E_g(T)$ is the band gap at a given temperature T, E_0 is the band gap at 0 K, and α and β are the constants. Here, we use $E_0 = 2.56$ eV, $\alpha = 0.000\,33$, and $\beta = 7.7 \times 10^6$. The temperature dependent band gap calculated using eq 7 is shown in Figure 8. The band gap decreases with increase in temperature.

Based on the third-order perturbation theory of resonance Raman scattering, the ratio of 2-LO and 1-LO intensities can be written as

$$I_{2LO}/I_{1LO} = (n(\omega) + 1)\left|\frac{M}{E_g(T) - (E_0 - 2E_p) - i\Gamma_e}\right|^2 \tag{8}$$

where $M = \langle\phi_2|H_{ep}|\phi_1\rangle$ is the electron−phonon matrix element, E_0 is the incident photon energy, E_p is the 1-LO phonon energy, and Γ_e is the width of the electronic state. Treating M and Γ_e as constants, the intensity ratio calculated using eq 8 is also shown in Figure 6. Note that the data and the calculated intensity ratio show good agreement. This implies that the observed increase in the intensity ratio as a function of laser power predominantly arises due to the T-dependence of the band gap. At the lowest laser power, the local temperature is close to room temperature, and hence the band gap of CdS is 2.43 eV which is higher than the excited photon energy. However, as the local temperature rises via increase in laser power, the band gap starts decreasing and approaches the excitation photon energy resulting in the observed resonance condition. This results in an increase in 2-LO to 1-LO phonon intensity and also the appearance of distinct 3-LO and 4-LO phonons. At the highest temperature of 700 K, the band gap closely matches the excitation photon energy, and the intensity of 2-LO becomes almost two times that of 1-LO phonon.

In conclusion, Raman spectroscopic studies have been performed on CdS nanoparticles at different laser powers. Notably, increase in laser power affects the growth of the size of the nanoparticles significantly. Resonant Raman scattering is achieved on the highest laser-power-heated area of the sample by matching the band gap of CdS with the excitation photon energy. With increase in laser power (local temperature), the ratio of the intensity of 2-LO to 1-LO is found to increase.

Acknowledgment. We acknowledge S. Kataria for obtaining optical micrographs. We thank Dr. C. S. Sundar for interest in the work and Dr. Baldev Raj for support and encouragement.

References and Notes

(1) Bagnall, D. M.; Chen, Y. F.; Zhu, Z.; Yao, T.; Koyama, S.; Shen, M. Y.; Goto, T. *Appl. Phys. Lett.* **1997**, *70*, 2230.

(2) Tang, Z. K.; Wong, G. K. L.; Yu, P.; Kawasaki, M.; Ohtomo, A.; Koinuma, H. *Appl. Phys. Lett.* **1998**, *72*, 3270.
(3) O'Regan, B.; Gratzel, M. *Nature* **1991**, *353*, 737.
(4) Colvin, V. L.; Goldstein, A. N.; Alivisatos, A. P. *J. Am. Chem. Soc.* **1992**, *114*, 5221.
(5) Ba Hoang, T.; Titova, L. V.; Jackson, H. E.; Smith, L. M.; Yarrison-Rice, J. M.; Lensch, J. L.; Lauhon, L. J. *Appl. Phys. Lett.* **2006**, *89*, 123123.
(6) Chuu, D.-S.; Dai, C.-M. *Phys. Rev. B* **1992**, *45*, 11805.
(7) Yakovlev, V. V.; Lazarov, V.; Reynolds, J.; Gajdardziska-Josifovska, M. *Appl. Phys. Lett.* **2000**, *76*, 2050.
(8) Abdi, A.; Titova, L. V.; Smith, L. M.; Jackson, H. E.; Yarrison-Rice, J. M.; Lensch, J. L.; Lauhon, L. J. *Appl. Phys. Lett.* **2006**, *88*, 043118.
(9) Wang, X. J.; Wang, L. L.; Huang, W. Q.; Tang, L. M.; Zou, B. S.; Chen, K. Q. *Semicond. Sci. Technol.* **2006**, *21*, 751.
(10) Leite, R. C.; Scott, J. F.; Damen, T. C. *Phys. Rev. Lett.* **1969**, *22*, 780.
(11) Sahoo, S.; Arora, A. K.; Sridharan, V. *J. Phys. Chem. C* **2009**, *113*, 16927.
(12) Arora, A. K.; Rajalakshmi, M.; Ravindran, T. R.; Sivasubramanianm, V. *J. Raman Spectrosc.* **2007**, *38*, 604.
(13) Gupta, R.; Xiong, Q.; Adu, C. K.; Kim, U. J.; Eklund, P. C. *Nano Lett.* **2003**, *3*, 627.
(14) Sivasubramanian, V.; Arora, A. K.; Premila, M.; Sundar, C. S.; Sastry, V. S. *Physica E* **2006**, *31*, 93.
(15) Dimitrov, R. I.; Moldovanska, N.; Bonev, I. K. *Thermochim. Acta* **2002**, *385*, 41.
(16) Campbell, I. H.; Fauchet, P. M. *Solid State Commun.* **1986**, *58*, 739.
(17) Goldstein, A. N.; Echer, C. M.; Alivisatos, A. P. *Science* **1992**, *256*, 1425.
(18) Park, K. *Phys. Lett. A* **1967**, *25*, 490.
(19) Sood, A. K.; Arora, A. K.; Umadevi, V.; Venkataraman, G.; Pramana, *J. Phys. (Paris)* **1981**, *16*, 1.
(20) Wang, R. P.; Xu, G.; Jin, P. *Phys. Rev. B* **2004**, *69*, 113303.
(21) Cheng, H.-M.; Lin, K.-F.; Hsu, H.-C.; Hsiehb, W.-F. *Appl. Phys. Lett.* **2006**, *88*, 261909.
(22) Sahoo, S.; Sivasubramanian, V.; Dhara, S.; Arora, A. K. *Solid State Commun.* **2008**, *147*, 271.
(23) Feng, Z. C.; Perkowitz, S.; Wrobel, J. M.; Dubowski, J. *Phys. Rev. B: Condens. Matter Mater. Phys.* **1989**, *39*, 12997.
(24) Luo, Y. Y.; Duan, G. T.; Li, G. H. *Appl. Phys. Lett.* **2007**, *90*, 201911.
(25) Ravindran, T. R.; Arora, A. K.; Balamurugan, B.; Mehta, B. R. *Nanostruct. Mater.* **1999**, *11*, 603.
(26) Tran, T. K.; Park, W.; Tong, W.; Kyi, M. M.; Wagner, B. K.; Summers, C. J. *J. Appl. Phys.* **1997**, *81*, 2803.

JP912103T